JOURNAL OF SPACECRAFT AND ROCKETS
Vol. 46, No. 1, January–February 2009

Characterization of Low-Density Open-Cell Foams for Space Inflatable Applications

Grazia Bitetti,* Sandro Mileti,* and Mario Marchetti†
University of Rome "La Sapienza," Rome, Italy 00184

DOI: 10.2514/1.23727

Many space agencies are oriented toward the use of inflatable technology for future-generation habitats and modules in an effort to reduce the overall weight, which in turn increases the weight payload that can be sent into orbit or in planetary transfer. These innovative habitats must provide a micrometeoroid and orbital debris protection. It is necessary to determine which polymeric foam material could be more adequate for the purpose. In this work, several open-cell foams were selected to be tested. Because the candidate foam must fulfill packaging and deployment operations and capture debris fragmentations, mechanical properties were evaluated. Furthermore, atomic oxygen surface exposure was performed on the foams to simulate low-Earth-orbit conditions in case of accidental direct exposure. This experimental investigation provides several basic results for selecting the most suitable foam for inflatable micrometeoroid and orbital debris protection.

Nomenclature

C_d = compression set expressed as a percentage of the original deflection
C_t = compression set expressed as a percentage of the original thickness
T_f = final thickness of the test specimen 40 min after the compression end
T_s = thickness of the used spacer bar
T_0 = original thickness of the test specimen

I. Introduction

THE future of space exploration focuses on manned long-duration missions through the use of the low-Earth-orbit (LEO) modules and moon/Mars base outposts. In this context, space inflatable technology takes place, resulting in several advantages with respect to the metallic counterpart.

The inflatable technology involves the use of lightweight flexible materials in space structure design, represented by polymeric and polyurethane thin films, fabrics, and low-density open-cell foams. These materials, much lighter than metals, can be bonded to each other by the use of adhesives or sewing techniques to set up a multilayer structure, each layer having a different function from the structural to the multilayer insulation protection. This technology permits the design of deployable structures, obtaining a significant weight reduction and the possibility to package them in much smaller volumes than the traditional systems, increasing the payload capacity and consequently reducing mission costs [1,2].

In the past, inflatable structures were used for space antennas, solar arrays, sunshields, and space suits. At present, a large interest has developed in the design of more complex structures such as habitat modules, containers, and fuel tanks for in situ storage [1–3]. For these types of structures, the micrometeoroids and orbital debris (MMOD) protection shield plays a fundamental role. This flexible shielding system is composed of several multilayers: a defined number of multishock bumpers for the projectile fragmentation and a high-strength rear wall to protect the underneath restraint and bladder layers of the inflatable module from puncture. Each multilayer bumper is conceived as separated and maintained in the final deployed position using a low-density-foam spacer. The foam is initially squeezed in the packaged configuration for launch and allowed to expand after achieving its final orbit.

The intent of this paper is to evaluate, through a test campaign, the mechanical properties of four different low-density open-cell foams to select the most suitable spacer for a flexible MMOD shield design. The four foam candidates are two polyimide, a melamine, and a polyurethane type. To finalize the inflatable habitat module design for LEO missions, the tests were completed by providing an analysis of atomic oxygen effects on the indicated foams. This chemical specie is indeed the most damaging factor constituting the neutral atmosphere in LEO. Its attack produces oxidation phenomena that compromise the integrity of the spacecraft's surfaces due to mass-loss and morphology changes. These effects result in thermal-optical-electrical degradation and erosion of the space materials. In case of damage of the MMOD shield, the foam will be exposed to atomic oxygen attack. The detrimental effect is investigated on the foam samples through the analysis of mass-loss results and related scanning electron microscopy (SEM). All of the tests were performed using dedicated mechanical testing machines and facilities developed at the Scientific Aerospace Solutions Laboratory (SASLab) of the Aerospace and Astronautic Department, University of Rome "La Sapienza."

II. Materials

Open-cell foams are extremely lightweight materials constituted by a continuous solid polymer in which void space cells are dispersed through the solid. These materials are typically 80–95% porous; due to its structure, it is remarkably stiff: the result is a very high strength-to-weight ratio. Foams have also good thermal insulation, buoyancy and energy dissipation [4,5]. In vacuum space environment, the open-cell structure results in rapid and complete air release. Taken together, the beneficial properties of open-cell foams not only guarantee good performance, but they also allow to reduce system mass and costs.

Regarding to the space inflatable applications, the open-cell foams are particularly suitable to realize the spacers among the Nextel bumpers and between the last bumper and the Kevlar rear wall in the MMOD shield. These support layers are typically formed from low-density, open-cell foams and are assigned to separate the bumpers from each other, maintaining bumper standoff while on orbit. The flexible shield is easily deployed by simply unfolding it and attaching it on top of the structure with the use of Velcro, snaps, straps, bungee cords, or other similar types of attaching techniques. The cored foam

Received 6 June 2006; revision received 13 January 2008; accepted for publication 2 May 2008.

*Aerospace Engineer, Aerospace and Astronautics Department, Via Eudossiana 18.
†Full Professor, School of Aerospace Engineering, Via Eudossiana 18.

layers used in five of the NASA TranHab MS experiments have contributed to the shielding by the fact that they fully support the Nextel layers. They also appear to mitigate lateral expansion of the debris cloud which results in smaller entry holes and reduced tearing within the Nextel layers. For this reason, the properties of open-cell foams must be investigated.

In the present work the main mechanical and environmental properties of four open-cell foams were analyzed, considering exactly two types of polyimide foams (Solimide AC 530 and Solimide AC 550), a melamine [Eurofoam (EF) 114], and a polyurethane foam type (EF 110/21/ET).

A brief description of the selected foams follows: The Solimide is a polyimide nonfibrous insulation foam, inherently fire resistant. This foam has a three-dimensional mesh structure and performs over a wide temperature operating range: it remains flexible from +200 to −200 °C. Because of the polyimide's high operating temperatures and also good cryogenic insulation properties, this type of foam can potentially reduce the amount of Thermal Protection System (TPS). The melamine open-cell foam is produced from melamine resin, a thermoset plastic from the aminoplastics group. Its characteristic feature is the delicate three-dimensional filigree network structure formed from slender and hence readily thermoformable filaments. The polyurethane foam is a mixture of several chemicals. The basic compounds are polyol, an organic compound with a high molecular weight and TDI (toluene di-isocyanurate), an organic compound of lower molecular weight than polyol. This type of foam is characterized by high mechanical damping, resistance to fracture during handling and launch and additionally provides a positive restoring force to its dimensions. Finally, these materials have extremely low thermal conductivity.

III. Foam Mechanical Characterization

The selected open-cell foams underwent a mechanical test campaign to evaluate the intrinsic material properties. At this purpose density, tensile and constant-deflection compression-set tests were performed, following the American Society for Testing and Materials (ASTM) international standards.

Density measurements were provided using BasicLite electronic precision balance (Sartorius AG) following the ASTM D3574 [6] test A method. For each material, 3 samples were cut, for a total of 12 tested specimens. Designated mean foam densities are listed in Table 1.

A. Tensile Tests

Tensile strength was measured using an Instron 3367 testing machine, which is provided with a HBM U2b force transducer. The tester works using a controlled displacement speed. The tests were conducted following the international standard ASTM D3574 test E. Dumbbell specimens with the nominal size of $139.7 \times 25.4 \times 12.5$ mm were realized to study the tensile strength of the open-cell foams. For each material, 3 samples were cut from flat sheet material. The foam rises in the thickness direction and the top and bottom surfaces are parallel and free of skin. Figure 1 shows a Solimide AC 530 specimen before and after the tensile test.

Experimental results are shown in Fig. 2, including four graphs, each displaying the force/elongation rate for each tested foam. The mean values of tensile strength, ultimate elongation and elongation at break are indicated in Table 2.

Results reveal that polyimide and melamine foams show an initial elastomeric trait but fail in the brittle regime, instead the polyurethane foam exhibits the elastomeric characteristic failure behavior. All foams fail due to an initial crack that propagates until failure occurs. Both types of polyimide open-cell foams results have very similar trends. The melamine foam presents more strength, but less stiffness than the polyimide and polyurethane, surely due to its intrinsic type of three-dimensional network structure. Its tensile strength results higher than the Solimide AC 550, although with similar density. Finally, the polyurethane EF 110/21/ET reveals to be the most performing foam, with high elongation at the break, compared with the others.

Table 1 Mean foam density results

Sample	Sample volume, mm^3	Density, g/m^3
Solimide AC 530	126.23	0.00622
Solimide AC 550	127.00	0.00844
EF 114	128.65	0.00885
EF 110/21/ET	129.53	0.01753

a) Undeformed specimen **b) Broken specimen**

Fig. 1 Solimide AC 530 sample before and after the tensile test.

B. Constant-Deflection Compression-Set Tests

The compression test on open-cell foams used for inflatable space applications is fundamental to evaluate the response of the material when it undergoes packaging and deployment, because these foams are usually used as spacers for the MMOD. These materials need to maintain, once deployed, their mechanical and geometrical properties.

During the launch sequence, the packaging/storage of the structure must not affect the performances of the foam because its duty is mainly based on its shape recovery. A possible low or not complete foam compression recovery cannot be acceptable because it will affect the final correct geometry, severely compromising the performance of the MMOD and so the outcome of the entire mission.

Constant-deflection compression-set tests were conducted following the international standard ASTM D3574-03 test D. The samples have parallel top and bottom surfaces and essentially perpendicular sides. For each material, three samples were tested. Compression specimens have nominal size $100 \times 100 \times 50$ mm (Fig. 3).

The tests were executed using a Schenck Trebel 100 traction/compression machine. The compression device consists of two flat plates realized in AISI 304 steel (Fig. 4) and held parallel to each other, with a series of holes for air spillage; the space between the plates is adjustable to the required deflection thickness controlled by a displacement transducer. The test method consists in deflecting the foam specimen to a specified deflection, exposing it to specified conditions of time and temperature and, finally, measuring the change in the thickness of the specimen after a specified recovery period.

The measurement of each sample was taken using a sliding caliper gauge with no contact with the foam and graduated to permit precise measurements within ±1% of the sample dimensions as indicated by the standards. The selected compression value is 90% of the original sample thickness; steady-state time is 22 h. The thickness recovery check was measured after 40 min.

It is well understood that the deformation of open-cell foams shows three main regimes: an initial linear elastic regime, in which the strain energy is stored in the reversible bending of the struts, a plateau regime, in which small increases in load lead to very large additional strain, and finally a densification regime in which the

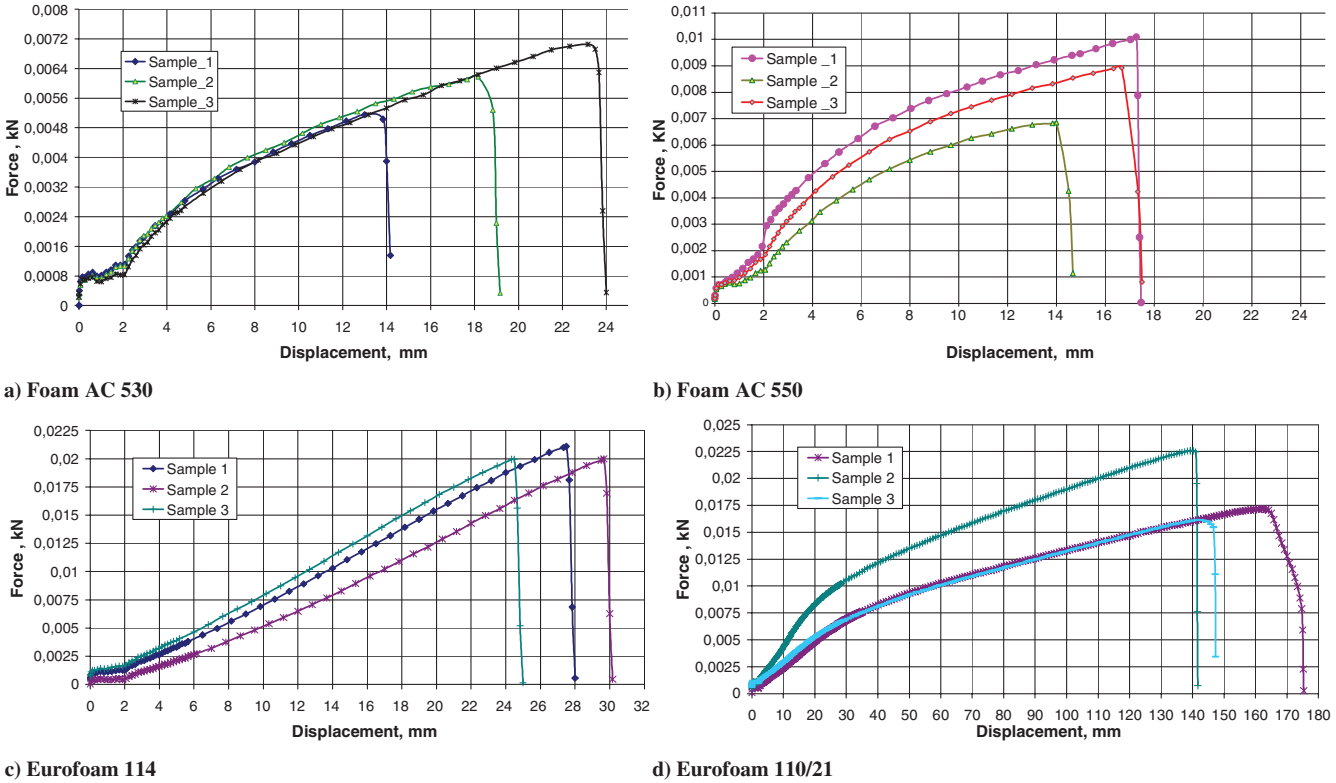

Fig. 2 Tensile tests graphics results for all open-cell foam samples.

reticular struts begin to impinge upon each other. At this last stage, the foam starts to exhibit a modulus approaching that of the solid material from which it is made. Results of the force-displacement curves for the uniaxial compression in the rise direction of the foams, evidencing the three regimes, is shown in Fig. 5.

In the Table 3 are reported the mean compression recovery results after 40 min. The results indicate that the melamine EF 114 has the best behavior in compression recovery. The polyurethane EF 110/21/ET looses around one third of the initial thickness, instead the polyimide open-cell foams fail the complete recovery target. The different behavior is related to the internal structure and density values of the different foams.

Other measurements of the thickness recovery were taken after several hours (up to 48 h) from the end of the compression. These additional measurements are not indicated in the ASTM standard, but considered useful for a complete recovery evaluation of the foams. The obtained values are indicated in Table 4. Analyzing Tables 3 and 4, we can notice that whereas the melamine foam recovers best and more quicker than the others after 40 minutes, the polyurethane foam has almost an identical complete recovery but in much longer time.

For open-cell foams the plateau region in the stress-strain curve leads to localized buckling, bending and collapse of the cell struts. Local collapse in these zones is terminated by contact between cell ligaments. In the process collapse spreads to neighboring cells which were up to that time intact. The spreading of collapse occurs at a well-defined load plateau and continues until most of the cells are thus affected when the material response regains stiffness once more. The relatively low initial stress peak and the extended plateau are defining

Fig. 3 Foam samples for the compression test.

features of the excellent energy absorption of such materials [7]. In our case the melamine foam reported the most extended plateau and the lowest initial peak (Fig. 5).

Figure 6a shows the three-dimensional skeletal structure with no membranes between strands of the melamine foam after undergoing the test. The SEM was taken from a most affected zone of the sample. The destruction of struts reveal to be very low justifying its excellent recovery behavior. Moreover, low number of collapses leads to intrinsic high buckling deflections of the struts which makes the foam capable to recover better from compressions.

It is commonly claimed that the initial linear elastic part of the stress-strain curve is the result of the bending of struts which are

Table 2 Tensile test results

Sample	Tensile strength, kPa	Standard deviation, %	Ultimate elongation, mm	Standard deviation, %	Elongation at break, %
Solimide AC 530	44.8	9.1	18.78	8.3	51.82
Solimide AC 550	63.1	7.8	16.78	7.1	48
EF 114	138.3	2.4	26.3	7.8	35
EF 110/21/ET	129.7	10.1	151.79	7.1	202

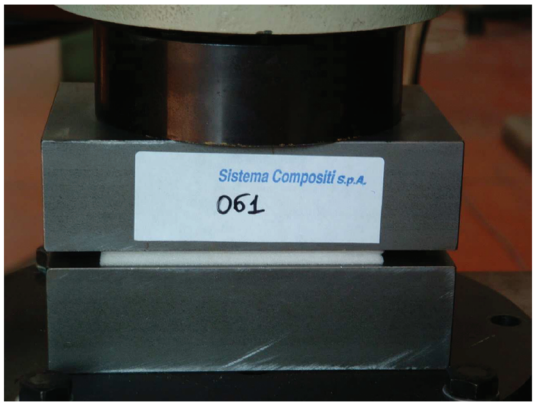

Fig. 4 Melamine EF 114 foam sample during the compression test.

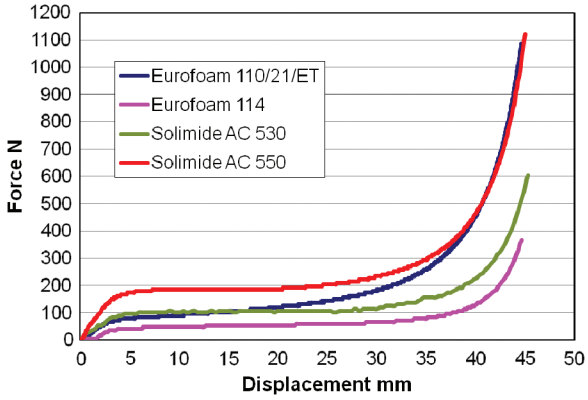

Fig. 5 Compression-set mean graphs of the tested samples.

oriented perpendicular to the load direction, whereas the plateau region of the stress-strain curve is the result of the "buckling" [7] of struts that are oriented parallel to the load direction. because the collapsing of the struts occur primarily in the plateau region, then the melamine struts are therefore capable of high buckling deflections.

Similar to the melamine foam also the polyurethane evidences (Fig. 6b) absence or very low strut ruptures. Its mechanistic interpretation can be related to the melamine one except for its higher stiffening (reaching 1100 N) which makes it more difficult to package into a small volume. The higher stiffening is mainly due to the larger cross-sectional area of the ligaments.

The low recovery exhibited by both Solimide AC 530 and AC 550 foams can be explained by the numerous ligament ruptures occurred.

Table 3 Compression recovery after 40 min

Sample	T_0, mm	T_f, mm	C_t, %	T_s, mm	C_d, %
Solimide AC 530	49	23	53.1	4.9	58.9
Solimide AC 550	49	16.5	66.3	4.9	73.7
EF 114	48.5	43.1	11.1	4.85	12.4
EF 110/21/ET	50	32.9	34.2	5	38

Table 4 Compression recovery after several hours

Sample	Original thickness, mm	After 3 h, mm	After 6 h, mm	After 48 h, mm
Solimide AC 530	49	26.7	27	32
Solimide AC 550	49	19.3	21.2	25.6
EF 114	48.5	45.6	45.7	47
EF 110/21/ET	50	44.5	45	46.6

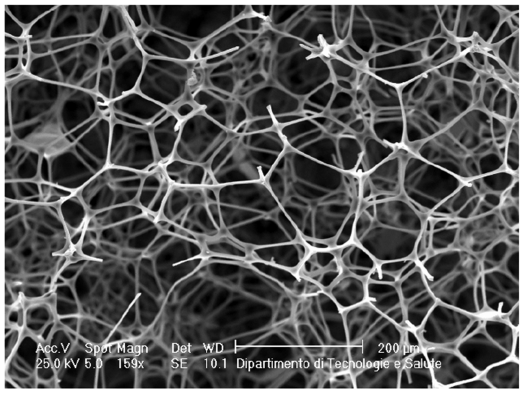

a)

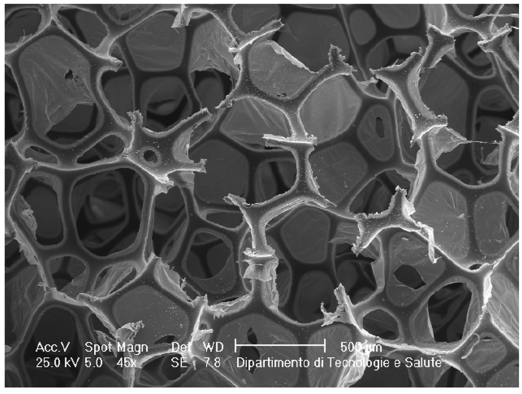

b)

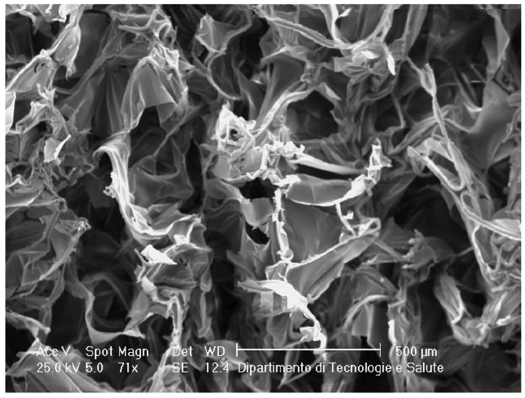

c)

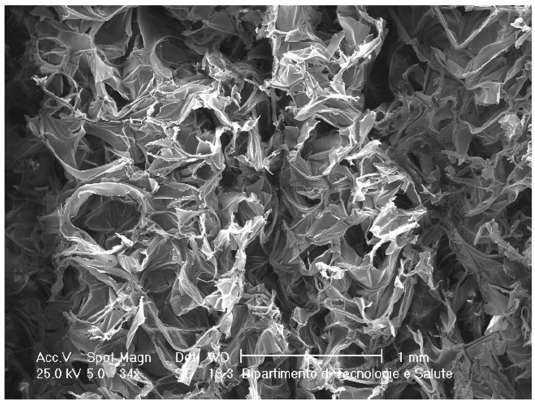

d)

Fig. 6 SEM images after compression test: a) melamine, b) polyurethane, c) Solimide AC 530, and d) Solimide AC 550.

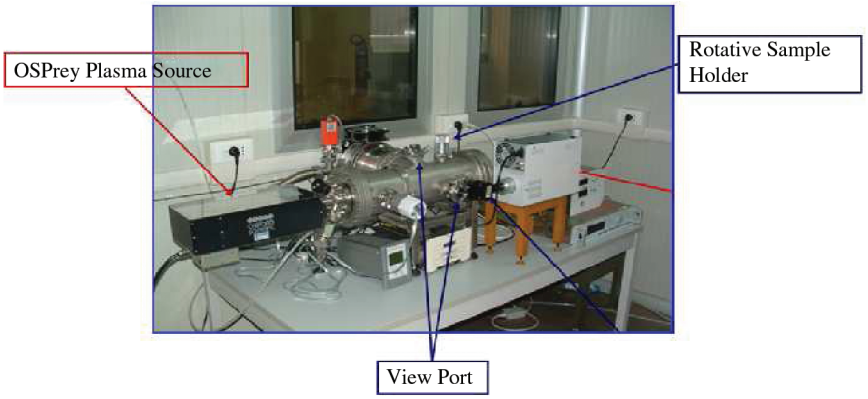

Fig. 7 Atomic oxygen simulator.

The SEM images (Figs. 6c and 6d) show how the cells and their faces are crumpled in complex patterns. It is clearly noticeable the permanent wavy deformation (Fig. 6d) on the local collapsed zone caused by the crushing effect. The stiffer response of the AC 550 foam is basically due to its higher cell density.

IV. Low-Earth-Orbit Foam Characterization

The typical LEO space environment includes several hazardous factors, including vacuum, thermal cycling, UV radiations, ionizing radiations (electrons, protons), micrometeoroids and orbital debris, and atomic oxygen [8–10]. Each of these physical phenomena is a damaging source for spacecraft materials: the high vacuum leads to outgassing effect, consisting in a mass loss due to the release of adsorbed or occluded gases in the material. The gradient due to the thermal cycles initiates a microcracking process inside the material, with consequent material weakening. The atomic oxygen interaction with materials produces oxidation, causing degradation of thermal-optical, electrical, and mechanical properties of the materials. Hydrocarbon-based materials undergo surface erosion due to the development of volatile oxidation products [11–13], resulting in mass-loss and material surface-morphology changes [14].

A. Atomic Oxygen Tests

With the considered open-cell foams in the role of a spacer, they are interposed between a Nextel or Kevlar multilayer in the MMOD configuration. Therefore, the foam layer is not in direct contact with the external LEO environment. If debris impacts the shield and penetrates the multilayer bumpers, damaging the MMOD, the foam will be exposed to the atomic oxygen attack. This detrimental effect, occurring on many advanced space materials, is investigated on the foam samples.

The atomic oxygen tests were executed using an Oxford Scientific plasma (OSPrey) source. The instrument is installed in a dedicated facility (the atomic oxygen simulator, shown in Fig. 7) and developed at the SASLab to simulate the material degradation in LEO. The maximum vacuum value achievable in the chamber is about 1×10^{-5} Pa.

The OSPrey plasma source (Fig. 8), produced by Oxford Scientific Instruments, is a radio-frequency inductively coupled plasma source. The operating principle is based on the ionization of the oxygen molecules by coupling the energy from a radio-frequency power source (13.56 MHz) to an ionized gas.

This instrument is constituted by an entirely stainless steel cylindrical tube in which the plasma is generated. The emission of the plasma occurs through a quartz aperture plate with a 23 mm diameter, containing 97 holes with a 0.2 mm diameter. The OSPrey plasma source generates an almost totally neutral oxygen beam, composed of 99% neutral elements (about 60% O atoms and about 40% O_2 molecules) and 1% O^+ ions. The plasma test conditions are indicated in Table 5. The spectrum emission radiation of the source at test power conditions (300 W) is illustrated in Fig. 9. It can be noticed that the UV irradiance is negligible, and so no bond dissociations, which lead to surface cracking or embrittlement, should be caused by the source radiation.

The tests were conducted following the international standard ASTM E2089 [15]. One sample was considered for each foam, but it was cut in $50 \times 50 \times 10$ mm dimensions to ease the sample cutting and minimize the mass-loss evaluation error. The sample surface was positioned at a normal incidence with respect to the atomic oxygen beam to simulate the worst colliding case.

B. Results and Discussion

For all samples tested at atomic oxygen attack, the mass-loss and surface-morphology changes were analyzed [14]. The mass-loss value achieved is crucial for the final evaluation of the best candidate. In fact, in the case of accidental perforation of the MMOD, the direct exposure could lead to a significant mass loss due to diffused erosion underneath the outer layers. This eventually brings a recession of the spacer's height and consequently weakens the MMOD protection. Instead, the surface morphology gives a detailed indication of the different erosion processes undergone by each foam.

The total mass loss of the material samples is analyzed using the gravimetric technique. The samples were weighed before and after the atomic oxygen exposure and their mass loss was calculated using a Sartorius BL-150S balance with a sensitivity of 1 mg. Consequently, the erosion yield was also calculated following the ASTM standard formula $\mathbf{E_S} = \Delta \mathbf{M_S}/(\mathbf{A_S}\boldsymbol{\rho}_\mathbf{S}\mathbf{F_k})$, where $\Delta \mathbf{M_S}$ is the sample mass loss, $\mathbf{A_S}$ is the surface exposed area, $\boldsymbol{\rho}_\mathbf{S}$ is the sample density, and $\mathbf{F_k}$ is the effective fluence on the Kapton witness material. The mass-loss and erosion-yield results for polyimide and melamine foams are indicated in Table 6. Inherent to the polyurethane foam, it is necessary to report that after 2 h of plasma

Fig. 8 OSPrey radio-frequency plasma source.

Table 5 Plasma test parameters

Experimental parameters	Values
Working pressure, pa	1×10^{-3}
Ion content, %	40
Plasma flux, neutral species/cm^2 · s	6.75×10^{15}
Total AO fluence, atoms/cm^2	1.463×10^{20}
Total fluence, neutral species/cm^2	3.11×10^{20}
AO energy, eV	5–25

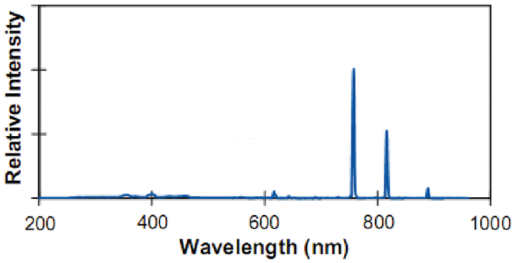

Fig. 9 Spectrum emission of the radio-frequency source.

oxygen exposure, the sample almost totally merged. The test was interrupted and it was impossible to carry out the mass-loss and the SEM analysis results. Observing the mass-loss values, the melamine foam presents a significant mass reduction. The polyimide foams behaved in a similar manner, with both the same characteristics and mass-loss percentage. These foams turned out to have better resistance than the other foams.

Because the Solimide open-cell foams contain imide groups and have a meshlike structure, the atomic oxygen action on this material is manifested by the formation of volatile oxide (CO and CO_2), with consequent mass loss and surface erosion. The SEM micrograph of the Solimide AC 530 foam before and after 8 h of exposure shown in Fig. 10 exhibits an etching effect caused by the atomic oxygen: the surface morphology of the Solimide foam changes significantly. The cells have decreased their dimensions, as has the thickness of the boundary ribs that surround the cells. The membranes that close some cells were removed, leaving the basic reticular structure of the material. The foam structure appears collapsed on itself, probably due to the oxygen plasma energy that raised the surface temperature to nearly 200°C, which is slightly lower than the continuous operative temperature of the foam (205°C).

Figure 11 shows a SEM micrograph of the Solimide AC 550 foam before and after 8 h exposure, in which the same erosion effect and shrinkage evidenced on the Solimide AC 530 sample is visible. The melamine has a different structure from the polyimide; in fact, its configuration is not a mesh type, but a network type. The cells are more regular and the structural branches are well defined; their shape is triangular and their average thickness is around 5 μm. Notice that no membranes surround the cells (Fig. 12a). Because of the melamine's intrinsic structure, the reaction to atomic oxygen attack differs from the other foams. A first macroscopic observation reveals a degraded brittle surface that is easily removable. Figures 12a and 12b show a SEM micrograph of the melamine EF 114 before and after 8 h of testing. After exposure, the structure seems to merge on itself and a structural collapse occurs, probably due to the surface temperature (nearly 200°C) that the plasma energy induced. The average branch thickness decreases at about 1.5 μm and frequently presents failure. Furthermore, it is evident (Fig. 13) that the ligament intersections of the network are eroded, and circular cavities are generated on the thinner areas, resulting in the starting point of the rupture.

As stated previously, the polyurethane EF 110/21/ET foam sample merged after 2 h of plasma oxygen exposure. The destructive effect is certainly due to the atomic oxygen beam and the energy reached on the surface during the testing. In fact, because the polyurethane is a thermosetting material, it softens with increasing temperature. In general, softening at high temperatures affects the polyurethane in two main ways: loss of mechanical properties and

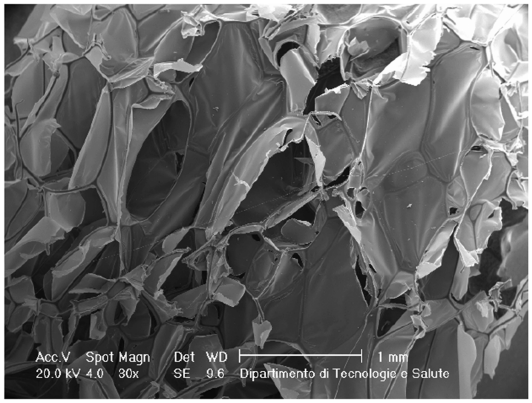

a) Unexposed sample

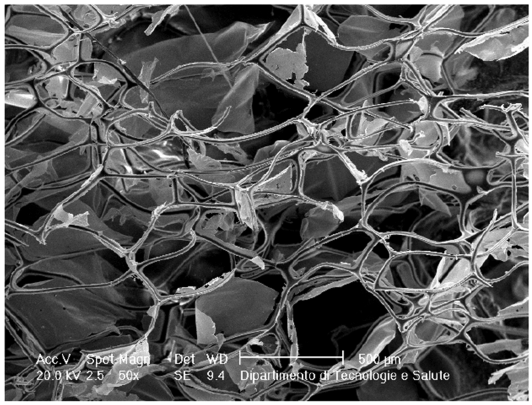

b) Exposed sample

Fig. 10 SEM image of the Solimide AC 530 sample before (30x) and after (50x) 8 h atomic oxygen exposure.

change in volume dimensions. In our case, the high temperature reached on the surface most probably melted the foam (melting temperature 70°C), making it impossible to determine the damaging contribution of the oxygen.

V. Conclusions

This research analyzed four types of open-cell low-density foams to characterize their mechanical and behavior for inflatable habitats' MMOD protection. Tensile tests proved that polyurethane and melamine foams have around 0.13 MPa tensile strength, an order of magnitude higher than with the polyimide foams. Obviously, the polyurethane foam also exceeds the elongation at the break, due to its elastomeric origin. More important is the compression-set recovery feature, which is a fundamental aspect for packaging and complete deployment of the structure. Tests reveal that the melamine foam exhibits the best compression and recovery performance, because its maximum compression resistance reaches nearly 400 N and loses only 3% of its initial thickness. The polyurethane also recovers well, but unexpectedly loses 6.8% of initial thickness only after 48 h. Both polyimide foam materials fail the complete recovery target.

Furthermore, to simulate the LEO environment, atomic oxygen plasma exposure was executed on the foams. A macroscopic consequence is that the polyimide and melamine foams have

Table 6 Mass loss and erosion results

Sample	Calculated density, kg/m^3	Average mass loss/area, g/ cm^2	Average mass loss, %	Erosion yield, cm^3/atom
Solimide AC 530	6.22	4.49E-4	6.18	4.93E-22
Solimide AC 550	8.44	8.23E-4	7.52	6.66E-22
EF 114	8.85	3.10E-3	27.04	2.39E-24
EF 110/21/ET	17.52	N.D.	N.D.	N.D.

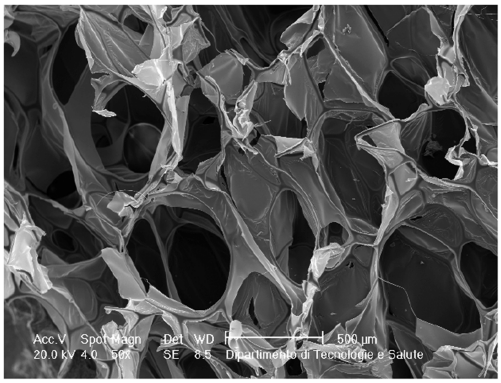

a) Unexposed sample

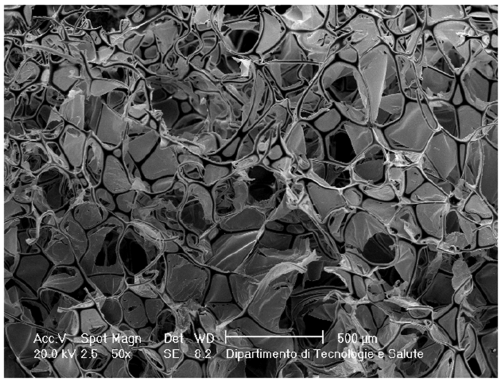

b) Exposed sample

Fig. 11 SEM image of the Solimide AC 550 sample before (50x) and after (50x) 8 h atomic oxygen exposure.

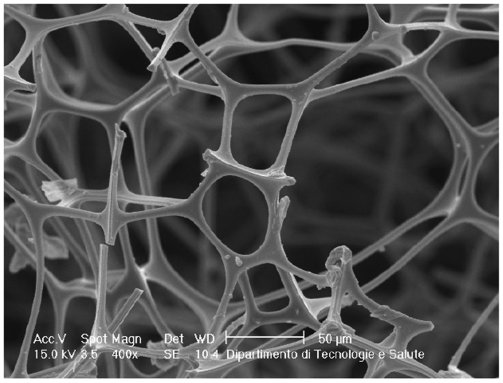

a) Unexposed sample

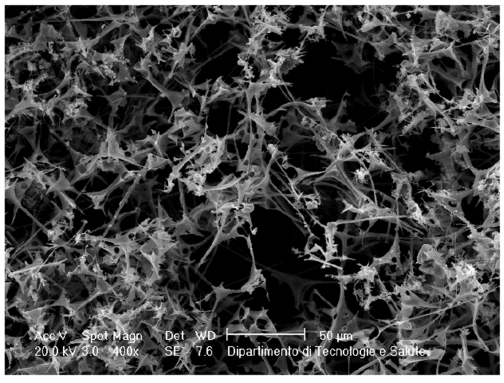

b) Exposed sample

Fig. 12 SEM image of the melamine EF 114 sample before (400x) and after (50x) 8 h atomic oxygen exposure.

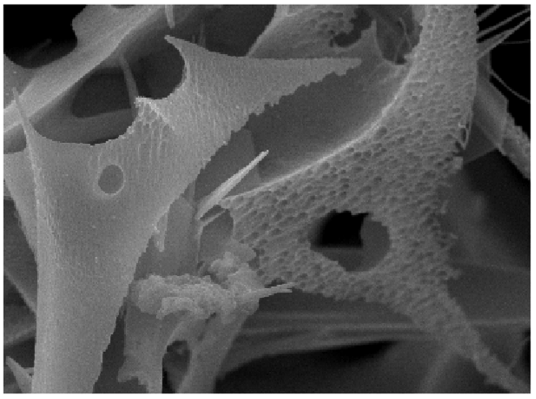

Fig. 13 Melamine EF 114 after (3000x) 8 h atomic oxygen exposure: morphology of AO erosion.

undergone a substantial change in surface-morphology aspect. The SEM analysis shows the leveling erosion effect on the polyimide mesh structure and cell-dimension reduction. Also, the melamine network structure was heavily eroded, losing parts of the structural ribs, and its surface deteriorated to a much more brittle material. A collapsing effect is visible on all tested foams, and this phenomenon is probably due to the oxygen-beam working temperature. The atomic oxygen effect is also valuable in terms of mass loss caused by the erosion phenomenon. Gravimetric results have evidenced a 27% mass loss for the melamine, compared with 6–7% for the polyimide foam. Because of the merging effect of the polyurethane, o related analyses were possible.

From an overall evaluation of the foams' behaviors through the test campaign, this work concludes that the most appropriate and efficient open-cell foam is the melamine. This choice is validated by its excellent mechanical attitude, regardless of the fact of its nonoptimal resistance to atomic oxygen.

Acknowledgments

The studies on the foams were conducted for the Italian Space Agency (ASI) Flexible Expandable Structure (FLECS) program, for which the main contractor is Alcatel Alenia Space (Italy). All materials for testing were supplied by the Sistema Compositi S.p.A. Company. We would like to thank the Italian Space Agency for the opportunity given to us in working in this program.

References

[1] Cadogan, D., Grahne, M., Mikulas, M., "Inflatable Space Structures: A New Paradigm for Space Structure Design," 49th International Astronautical Congress, Melbourne, Australia, International Astronautical Foundation, Paper 98-I.1.02, 1998.

[2] Cassapakis, C., and Mitch, T., " Inflatable Structures Technology Development Overview," AIAA Paper 95-3738, 1995.

[3] Cadogan, D., Stein, J., Grahne, M., "Inflatable Composite Habitat Structures for Lunar and Mars Exploration," 49th International Astronautical Congress, Melbourne, Australia, International Astronautical Foundation Paper 98-13.2.04, 1998.

[4] Williams, M. K., Weiser, E. S., Fesmire, J. E., Grimsley, B. W., Smith, T. M., Brenner, J. R., Nelson, G. L., "Effects of Cell Structure and Density on the Properties of High Performance Polyimide Foams," *Polymers for Advanced Technologies*, Vol. 16, Jan. 2005, pp. 167–174. doi:10.1002/pat.567

[5] Weiser, E. S., Grimsley, B. W., Pipes, B. B., Williams, M. K., "Polyimide Foams from Friable Balloons," NASA TR-2002-47, 2002.

[6] "Standard Test Methods for Flexible Cellular Materials-Slab, Bonded and Molded Urethane Foams," American Society for Testing and Materials, Standard D3574, West Conshohocken, PA, 2003.

[7] Gong, L., Kyriakides, S., and Jang, W.-Y., "Compressive Response of Open-Cell Foams Part 1: Morphology and Elastic Properties, *International Journal of Solids and Structures* Vol. 42, Nos. 5–6, 2005 pp. 1355–1379. doi:10.1016/j.ijsolstr.2004.07.023

[8] Reddy Raja, M., "Review Effect of Low Earth Orbit Atomic Oxygen on Spacecraft Materials," *Journal of Materials Science*, Vol. 30, No. 2, 1995, pp. 281–307.
doi:10.1007/BF00354389

[9] Chambers, A. R., Harris, I. L., Roberts, G. T., "Reactions of Spacecraft Materials with Fast Atomic Oxygen," *Materials Letters*, Vol. 26, No. 3, 1996, pp. 121–131.
doi:10.1016/0167-577X(95)00261-8

[10] Banks, B. A., De Groh, K. K., Miller, S. K., "Low Earth Orbital Atomic Oxygen Interactions with Spacecraft Materials," NASA TM-2004-213400, 2004.

[11] Grossman, E., Gouzman, I., "Space Environment Effects on Polymers in Low Earth Orbit," *Nuclear Instruments and Methods in Physics Research, Section B: Beam Interactions with Materials and Atoms*, Vol. 208, Aug. 2003, pp. 48–57.
doi:10.1016/S0168-583X(03)00640-2

[12] Minton, T. K., Garton, D., "Dynamics of Atomic-Oxygen-Induced Polymer Degradation in Low Earth Orbit," *Chemical Dynamics in Extreme Environments*, Advanced Series in Physical Chemistry, Vol. 11, World Scientific, Singapore, 2001, pp. 420–489.

[13] Silverman, E. M., "Space Environmental Effects on Spacecraft: LEO Materials Selection Guide," NASA CR 4661, 1995.

[14] Bitetti, G., Carnà, E., Marchetti, M., Pilloni, L., Poscente, F., and Scaglione, S., "Effects of Atomic Oxygen Erosion on Space Materials," *Proceedings of the 5th International Symposium on Environmental Testing for Space Programmes*, SP-558, European Space Research and Technology Centre, Noordwijk, The Netherlands, Aug. 2004, p. 637.

[15] *Standard Practices for Ground Laboratory Atomic Oxygen Interaction Evaluation of Materials for Space Applications*, American Society for Testing and Materials, Standard E2089, West Conshohocken, PA, 2000.

D. Edwards
Associate Editor